Crucial Role of an Idiosyncratic Insertion in the Rossman Fold of Class 1 Aminoacyl-tRNA Synthetases: The Case of Methionyl-tRNA Synthetase[†]

Dominique Fourmy, Yves Mechulam,* and Sylvain Blanquet

Laboratoire de Biochimie, Unité de Recherche Associée No. 1970 du Centre National de la Recherche Scientifique, Ecole Polytechnique, F-91128 Palaiseau Cedex, France

Received July 11, 1995; Revised Manuscript Received September 14, 1995[⊗]

ABSTRACT: A few aminoacyl-tRNA synthetases are characterized by their ability to tightly bind a zinc atom. In the case of *Escherichia coli* methionyl-tRNA synthetase, a peptide of 21 residues (138−163) having a stable 3-D structure in solution is responsible for zinc binding [Fourmy, D., Meinnel, T., Mechulam, Y., & Blanquet, S. (1993) *J. Mol. Biol. 231*, 1066−1077; Fourmy, D., Dardel, F., & Blanquet, S. (1993) *J. Mol. Biol. 231*, 1078−1089]. This peptide, which belongs to a region connecting the two halves of the nucleotide-binding domain of methionyl-tRNA synthetase, is likely to form a modular domain close to the active center of the enzyme. In this study, two residues of the zinc-binding module, Asp138 and Arg139, are shown to contribute to the stabilization of the transition state of the reaction leading to the activation of methionine. Moreover, another residue, Phe135, located at the surface of the zinc-binding domain, is found to possibly guide the tRNA acceptor stem toward the active site of the enzyme during catalysis. The available data indicate an important functional role for the zinc-binding module of methionyl-tRNA synthetase, as well as for other modules connecting conserved secondary structure elements in the aminoacyl-tRNA synthetase family. The relation between the occurrence of such variable peptide modules and the expression of both substrate specificity and catalytic efficiency is discussed.

The catalytic specificity and efficiency of aminoacyl-tRNA synthetases (aaRS)[1] are key features of the translation process. The structure−function studies of this class of enzymes have benefited from the combination of genetic, biochemical, and structural approaches [see Meinnel et al. (1995), for a recent review]. Despite the apparent lack of resemblance between these isofunctional enzymes, the identification of short stretches of conserved sequences combined with the resolution of several aaRS structures led to the partition of aaRS into two classes thought to reflect the occurrence of two distinct ancestors (Eriani et al., 1990). One key feature distinguishing the members of the two classes is the structural arrangement of their catalytic center domain. This domain is indeed built around either a Rossmann fold (Rossmann et al., 1974) for class 1 aaRS or an anti parallel β sheet for class 2 aaRS. Taking into account such constant arrangements, the evolution of aaRS within each class to express specificity toward cognate amino acid and tRNA remains an intriguing problem. Within the catalytic domain, idiosyncratic peptide insertions were observed between conserved secondary structure elements (Cusack et al., 1991; Eriani et al., 1990; Starzyk et al., 1987). It is tempting to believe that such inserted peptides are involved in the expression of the specificity of each aaRS toward its amino acid and the acceptor arm of its cognate tRNA [see for instance Rould et al. (1989)]. Moreover, aaRS are modular enzymes, with one or two domains in addition to the catalytic center domain. These additional domains, the structures of which vary with the aaRS species under consideration, appear responsible for the specific recognition of tRNA regions distant from the acceptor stem, usually the anticodon loop [see Mechulam et al. (1995) for a review].

Another feature distinguishing a few aaRS from the other aaRS species is the occurrence of tightly bound zinc. In such cases, a part or all of the zinc ligands is (are) found in the above idiosyncratic insertions, inside the catalytic domain. The only exception to this behavior is *Escherichia coli* IleRS, for which one of the two zinc-binding sites was mapped outside of the catalytic center domain (Landro & Schimmel, 1994). This second zinc-binding region was nevertheless proposed to interact with the active site (Landro et al., 1994). Although in all studied cases the presence of the zinc ion was required for enzyme activity, the precise role of this metal has still to be described.

Methionyl-tRNA synthetase from *E. coli*, a homodimeric class 1 enzyme, contains one tightly bound zinc ion per protomer (Mayaux & Blanquet, 1981; Posorske et al., 1979). Protein denaturation is required to remove this metal (Mayaux et al., 1982), which is tetracoordinated by four cysteine residues (Cys 145, 148, 158, and 161) belonging to a Cys-X_2-Cys-X_9-Cys-X_2-Cys sequence (Cys motif; Fourmy et al., 1993b; Landro & Schimmel, 1993). This sequence resembles the zinc-binding sites of various nucleic acid binding proteins (Berg, 1990). In MetRS, the zinc motif is carried by connective polypeptide 1, an idiosyncratic insertion between the two halves of the Rossmann fold (Starzyk et al., 1987; see Figure 1). Mutation into Ala of either Cys in the above motif resulted in MetRS species from which the metal could be removed without denaturation. The study

[†] This work was supported in part by grants from the Fondation pour la Recherche Médicale and the Interface Chimie-Biologie program of CNRS.

* Author to whom all correspondence should be addressed. E-mail: yves@botrytis.polytechnique.fr.

[⊗] Abstract published in *Advance ACS Abstracts,* November 15, 1995.

[1] Abbreviations: aaRS, aminoacyl-tRNA synthetase; EDTA, ethylenediaminetetraacetate; a particular aaRS is abbreviated by the name of its cognate amino acid in the three-letter code followed by RS, e.g., MetRS, methionyl-tRNA synthetase.

0006-2960/95/0434-15681$09.00/0

FIGURE 1: Comparison of the connective polypeptides 1 of three class 1 aaRS. The molecules are drawn such that the Rossman folds have the same orientations. In the three cases, the connective polypeptide 1 is drawn in green. A, *E. coli* MetRS (Brunie et al., 1990). The positioning of the zinc-binding peptide (NMR structure, red line) within the crystallographic structure of MetRS is tentative and is based on the structural alignment previously described (Fourmy et al., 1993a). The yellow sphere represents the zinc ion. The residues of this peptide studied here, D138, R139, F140, F145, and K147, are drawn in blue. Only the active site domain of MetRS (residues 1−360) is shown. The thin green line represents the region of connective polypeptide 1 currently being revised. The ATP molecule is shown with the ball-and-stick representation. B, *E. coli* GlnRS active site domain (Rould et al., 1989). C, *B. stearothermophilus* TyrsRS active site domain (Brick et al., 1989). The figure was drawn using the Molscript program (Kraulis, 1991).

of such mutated enzymes led to the conclusion that the zinc ion, through its coordination by the four Cys, contributes to the correct folding of a part of the region surrounding the catalytic center of MetRS (Fourmy et al., 1993b). Because the 3-D model of the corresponding region in the MetRS crystallographic structure is currently being revised, the structure of a MetRS peptide encompassing the above Cys motif and capable of binding zinc was studied by using NMR (Fourmy et al., 1993a). Its 3-D structure is made of a series of four tight turns constrained by the zinc ion, thus resembling the metal-binding site of rubredoxin and of *gag* retroviral proteins. A model for the zinc-binding region of MetRS, which tentatively placed the zinc atom in the vicinity of the active site of MetRS, was derived from a partial alignment of the NMR and crystallographic (Brunie et al., 1990) structures (Fourmy et al., 1993a). From the whole data, it was suggested that the zinc ion might contribute to the spatial positioning of residues important for the catalysis.

The aim of the present study is to characterize such important residues implied by the above hypothesis. For this purpose, the M547 fully active monomeric form of the *E. coli* MetRS (Mellot et al., 1989) was used as a template to direct mutations of residues selected on the basis of the available structural data. Functional analysis of the produced mutants enables conclusions to be drawn on the contribution of zinc to the activity and specificity of MetRS.

MATERIALS AND METHODS

(A) Site-Directed Mutagenesis and Purification of MetRS Variants. Mutant genes encoding variants of the M547 form of MetRS were generated through oligonucleotide site-directed mutagenesis, as described elsewhere (Mellot et al., 1989). These genes were introduced in the pBSM547+ vector (Fourmy et al., 1993b) under the control of the *lac* promoter. Production of the M547 variants in the presence of IPTG (0.3 mM) was in JM101Tr cells (Hirel et al., 1988).

MetRS variants were prepared homogeneous as described (Meinnel et al., 1991) by two chromatographic steps, first on Superose-6 molecular sieves (Pharmacia; 1.6 × 50 cm) and second on a Q-Hiload anion exchanger (Pharmacia; 1.6 × 10 cm; 2.5 mL/min; 100 mM of KCl/h). Enzyme concentrations were calculated using the molar extinction coefficient at 280 nm of the trypsin-modified MetRS (1.72 cm^2/mg; Cassio & Waller, 1971). Phenylmethylsulfonyl fluoride (10^{-4} M) was systematically added to the buffers

during the purification to prevent proteolysis of native dimeric MetRS of chromosomal origin.

(B) Atomic Absorption Spectroscopy. Zinc atomic absorbancies were measured at 213.9 nm in the peak height mode during 5 s after 0.1 mL injections, using a Varian AA775 spectrophotometer equipped with an air−acetylene burner (Mayaux & Blanquet, 1981). Prior to analysis, MetRS variants were dialyzed overnight at 4 °C (Visking dialysis tubing, 12 000−14 000 Da cutoff) against buffer A [20 mM Tris−HCl (pH 7.5), 10 mM 2-mercaptoethanol, 100 mM KCl, 0.1 mM EDTA]. Standard solutions containing various zinc concentrations (5−50 μM) were prepared by dilution of a 15.3 mM $ZnCl_2$ solution in buffer A (Merck, Darmstadt, Germany).

(C) Isotopic [^{32}P]PPi−ATP Exchange and tRNA Aminoacylation Activity Measurements. Methionine-dependent [^{32}P]-PPi−ATP exchange activity was measured at 25 °C in standard buffer: 20 mM Tris−HCl (pH 7.6), 7 mM $MgCl_2$, 10 mM 2-mercaptoethanol, 0.1 mM EDTA, containing 2 mM [^{32}P]PPi, 2 mM ATP, and 2 mM methionine (Blanquet et al., 1974). For K_m measurements, ATP or methionine was varied from 0.05 to 2 mM or from 0.002 to 4 mM, respectively.

Aminoacylation assays for the determination of the K_m of methionine (Lawrence et al., 1973) were performed in the same standard buffer plus 150 mM KCl, 2 mM ATP, 0.5−50 μM [^{14}C]-L-methionine (1.8 TBq/mol; Dositek, France), and an amount of a crude tRNA extract of $tRNA_f^{Met}$ overproducing cells such that the final concentration of methionine accepting tRNA in the assay was 8 μM (Meinnel et al., 1988, 1991); this tRNA extract accepted 600 pmol of methionine per A_{260} unit. For the determination of the K_m of $tRNA_f^{Met}$, the concentration of [^{14}C]-L-methionine was 24 μM and the concentration of $tRNA_f^{Met}$ was varied between 0.5 and 20 μM. Prior to the reaction, stock solutions of enzymes in 10 mM potassium phosphate (pH 7.3), 10 mM 2-mercaptoethanol, and 55% (v/v) glycerol were diluted in 20 mM Tris−HCl (pH 7.6), 10 mM 2-mercaptoethanol, 0.1 mM EDTA, containing 200 μg of bovine serum albumine/mL. All enzymatic assays (100 μL final volume) were initiated by the addition of 25 μL of enzyme dilution.

(D) Fluorescence at Equilibrium. Variations of the intrinsic fluorescence of MetRS upon titration with substrates were followed as described (Blanquet et al., 1973, 1974; Fayat et al., 1977), at 25 °C, in buffer containing 20 mM Tris−HCl (pH 7.6), 10 mM 2-mercaptoethanol, 2 mM $MgCl_2$, and 0.1 mM EDTA. Titrations were achieved by successively adding to the 800 μL enzyme solution 5 μL aliquots of the studied substrate at increasing concentrations. From this, both the fluorescence upon saturation by the substrate and the dissociation constant could be determined. In the case of titration with $tRNA_m^{Met}$ [1500 pmol of methionine acceptance per A_{260} unit, prepared as described in Meinnel et al. (1993)], an optimal $MgCl_2$ concentration of 8 mM was used. In the case of titration of the MetRS variants studied with methionine or methioninol in the presence or in the abence of synergistic partners, the relative enhancements of intrinsic enzyme fluorescence upon saturation by the substrate (12%−27% depending on the enzyme variant considered and the substrates used) were lower than in the case of authentic M547 enzyme (30%−58%, depending on the substrate). Therefore, an enzyme concentration of 4 μM (instead of 0.8 μM for M547) was used in the titrations in order to increase the signal to noise ratio of the fluorescence signal.

Scheme 1

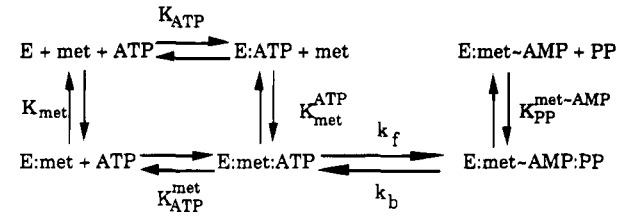

(E) Pre-Steady-State Studies. When the enzyme is mixed with combinations of methionine, ATP, and PPi in the presence of magnesium ions, the protein fluorescence varies exponentially (Blanquet et al., 1972; Hyafil et al., 1976). Fluorescence measurements at the pre-steady-state were performed using a stopped-flow apparatus described in Hyafil et al. (1976) in 20 mM Tris−HCl (pH 7.6) containing 0.1 mM EDTA, 10 mM 2-mercaptoethanol, and 2 mM $MgCl_2$. The formation of methionyl adenylate was started by mixing (1:1 v/v) an enzyme solution (2 μM) containing methionine (4 mM) and buffering pyrophosphate (10 μM) with another solution containing methionine (4 mM), pyrophosphate (10 μM), and various concentrations of the stoichiometric ATP−Mg^{2+} complex. For the reverse reaction, the preformed enzyme:methionyl adenylate complex, obtained by incubating the enzyme in the presence of 4 mM methionine and an appropriate concentration of ATP−Mg^{2+} (see Table 5), was mixed (1:1, v/v) with a solution containing the same concentrations of methionine and ATP−Mg^{2+} plus various amounts of stoichiometric PPi−Mg^{2+} complex.

Kinetic parameters (k_f and k_b) and equilibrium parameters (K_{ATP}^{Met}, K_{met}^{ATP}, and $K_{PP}^{met\sim AMP}$) of the methionine activation reaction (Scheme 1) are those defined in Hyafil et al. (1976). Their values were drawn from fits of the measured rate constants to the theoretical equation (Hyafil et al., 1976; Schmitt et al., 1994) using the MC-Fit program (Dardel, 1994).

RESULTS

(A) Residues Asp138 and Arg139, Located Upstream from the Cys Motif, Are Important for MetRS Activity. The tentative model positioning the zinc-binding peptide inside the catalytic core of MetRS is shown on Figure 1. It indicates that D138, R139, K142, K147, and K149 may have side chains located at the border of the active site crevice. These residues were therefore selected for further analysis. F135 was also selected because an aromatic residue (Tyr) is conserved at the corresponding position in the sequence of *Saccharomyces cerevisiae* MetRS (Figure 2A). Finally, F140, which is involved in the hydrophobic core of the Zn-binding peptide isolated from MetRS (Fourmy et al., 1993a), was also included in our analysis.

The genes of the MetRS variants corresponding to the F135L, D138A, R139A, F140L, K142Q, K147A, and K149A substitutions (Figure 2B) were constructed by site-directed mutagenesis of the *metG*547 gene. Their products were purified to homogeneity, and kinetic parameters for the [^{32}P]-PPi−ATP exchange and tRNA aminoacylation reactions were measured (Tables 1 and 2).

Regarding the maximal rates of the [^{32}P]PPi−ATP exchange and tRNA aminoacylation reactions, the studied

A

E.coli 133GMF**LPDRFVKGTCPKC**KSPDQY**GDNCEVCGA**
S.cerevisiae 325NSY**LADRYVEGECPKC**HYDDAR**GDQCDKCGA**

B

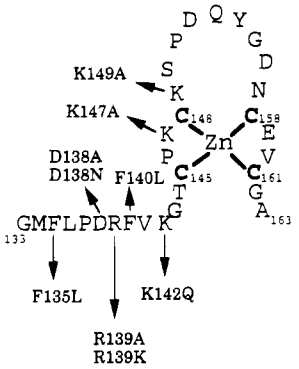

FIGURE 2: A, Alignment of the sequences of the Cys motifs of *E. coli* (Dardel et al., 1984) and *Saccharomyces cerevisiae* (Walter et al., 1983) methionyl-tRNA synthetases. Conserved residues are indicated in bold-faced characters. The numbering refers to the positions in the corresponding MetRS sequences. B, The different substitutions realised in the present study are indicated. The four cysteines binding the zinc ion are bold-faced.

Table 1: Michaelian Parameters of the [^{32}P]PPi−ATP Isotopic Exchange Reaction Catalyzed by the MetRS Variants[a]

	K_m (met) (μM)	V_m/[Et] (s^{-1})	K_m ATP (mM)	V_m/[Et] (s^{-1})
M547	22 ± 2	50 ± 2	0.30 ± 0.03	50 ± 5
F135L	7.5 ± 0.8	43 ± 3	0.42 ± 0.05	56 ± 5
D138A	190 ± 20	0.45 ± 0.03	1.0 ± 0.2	0.7 ± 0.1
D138N	110 ± 10	1.7 ± 0.1	0.66 ± 0.09	2.4 ± 0.3
R139A	30 ± 3	0.012 ± 0.001	0.31 ± 0.04	0.012 ± 0.001
R139K	88 ± 7	0.050 ± 0.004	0.90 ± 0.15	0.063 ± 0.007
F140L	180 ± 20	30 ± 2	0.7 ± 0.1	35 ± 4
K142Q	34 ± 3	38 ± 2	0.6 ± 0.1	46 ± 5
K147A	35 ± 4	60 ± 3	0.30 ± 0.04	60 ± 5
K149A	30 ± 4	64 ± 3	0.34 ± 0.03	70 ± 6

[a] The values were determined from standard assays, using homogeneous enzymes. K_m of methionine and of ATP and associated maximal rates (V_m) values, as well as standard errors, were derived from iterative nonlinear least-squares fits of the Michaelis−Menten equation to the measured initial rate values (Dardel, 1994).

mutants could be classified into three groups. First, the D138A and R139A variants showed, as compared to the wild type M547, a decrease of 2 and 3 orders of magnitude, respectively, of their V_m values in both the exchange and the tRNA aminoacylation reactions. The K_m values of methionine with the D138A variant in both the [^{32}P]PPi−ATP exchange and the tRNA aminoacylation reactions were significantly higher than those measured with the M547 enzyme. In addition, the K_m value of $tRNA_f^{Met}$ in the aminoacylation reaction catalyzed by D138A was 3-fold lower than that recorded with the M547 control. Second, in the case of the F135L variant, the V_m value of the aminoacylation reaction was slowed down by a factor of 15 with a concomitant increase of the K_m value of $tRNA_f^{Met}$ by a factor greater than 20. In contrast, the parameters of the [^{32}P]PPi−ATP exchange reaction were only slightly modified. Therefore, the substitution of Phe135 by Leu specifically affected the aminoacylation step. Third, modifications of Phe 140, Lys 142, Lys 147, or Lys 149 only slightly affected the [^{32}P]PPi−ATP exchange and aminoacylation

Table 2: Michaelian Parameters of the $tRNA_f^{Met}$ Aminoacylation Reaction Catalyzed by MetRS Variants[a]

	K_m(met) (μM)	V_m/[Et] × 10^3 s^{-1}	K_m $tRNA_f^{Met}$ (μM)	V_m/[Et] × 10^3 s^{-1}
M547	6.5 ± 1.2	3400 ± 400	2.3 ± 0.1	3300 ± 100
F135L	0.5 ± 0.2	45 ± 3	50 ± 20	240 ± 60
D138A	50 ± 17	37 ± 10	<0.5	22 ± 2
D138N	21 ± 5	210 ± 30	<0.5	120 ± 10
R139A	10.4 ± 1.6	0.85 ± 0.08	1.4 ± 0.4	0.69 ± 0.06
R139K	30 ± 7	3.7 ± 0.7	<0.5	1.7 ± 0.15
F140L	23 ± 5	1700 ± 240	0.9 ± 0.1	700 ± 40
K142Q	5.0 ± 0.5	3500 ± 300	5.7 ± 1.1	3800 ± 300
K147A	6.7 ± 1.3	2500 ± 300	4.9 ± 0.6	4300 ± 600
K149A	7.7 ± 0.9	3200 ± 200	3.5 ± 0.6	4400 ± 400

[a] The values were determined from standard assays using homogeneous enzymes. K_m of methionine and associated maximal aminoacylation rates (V_m) values, as well as standard errors, were derived from iterative nonlinear least-squares fits of the Michaelis−Menten equation to the measured initial rate values.

reaction parameters. The results concerning the K142Q variant agreed with those previously reported for a K142A variant (Ghosh et al., 1991).

The D138N and R139K variants were also constructed and purified to homogeneity for determination of their Michaelis−Menten parameters. As shown in Tables 1 and 2, the effects of these substitutions were very close to those caused by the substitution of D138 into alanine, thereby indicating the importance of the negative charge carried by Asp138.

After dialysis against a buffer containing the chelating agent EDTA (0.1 mM, see Materials and Methods), all enzyme variants retained zinc in a 1:1 stoichiometry. It could therefore be excluded that the observed variations of the kinetic parameters resulted from a measurable weakening of the binding of zinc. In addition, this result indicated that the introduced mutations caused no major structural change of the zinc-binding site.

(B) Mutations Upstream from the Zinc-Binding Motif Do Not Preclude Substrate Binding. In order to probe further the characteristics of the above MetRS mutants, their ability to accommodate substrates was evaluated. The strength of positive coupling between the methionine (met) and ATP sites was also examined because of its importance in the formation of the E:met:ATP−Mg^{2+} reactive complex (Blanquet et al., 1975; Fayat et al., 1977). This coupling is believed to compensate for the repulsion expected from the negative charges carried by the carboxylate of methionine and the α-phosphoryl group of ATP and thereby to drive the substrates toward the transition state (Hyafil et al., 1976). The free energy of coupling between the two sites can indeed be made measurable upon the suppression of one of these two negative charges when following the effect of the occupation of the methionine site on ATP−Mg^{2+} binding and *vice versa*. For instance, methioninol can be used in the place of methionine, or a combination of adenosine plus PPi−Mg^{2+} can mimic the ATP−Mg^{2+} molecule devoid of the α-phosphate charge.

The results of spectrophotofluorimetric titrations (Tables 3 and 4) showed that the affinity constants of all the studied mutants toward methionine or methioninol remained comparable to those measured with the M547 control enzyme within factors never exceeding 5.

The binding of methionine was further studied in the presence of adenosine or of adenosine plus PPi−Mg^{2+},

Table 3: Equilibrium Parameters of the Binding of Methionine to the Variants of Methionyl-tRNA Synthetase[a]

	K_{met} (μM)[b]	K_{met}^{ado}(μM)[c]	C_{met}^{ado} (kcal/mol)	K_{met}^{adoPP}(μM)[e]	C_{met}^{adoPP} (kcal/mol)[f]
M547	55 ± 5	11 ± 2	1.0	0.2 ± 0.1	2.4
F135L	13 ± 2	1.8 ± 0.2	1.2	0.05 ± 0.02	2.1
D138A	190 ± 60	55 ± 20	0.7	40 ± 8	0.2
D138N	180 ± 50	47 ± 20	0.8	9.0 ± 1.5	1.0
R139A	86 ± 15	32 ± 10	0.6	31 ± 5	0.0
R139K	80 ± 20	18 ± 3	0.9	16 ± 2	0.1
F140L	140 ± 30	35 ± 7	0.8	2.2 ± 0.2	1.6
K142Q	35 ± 5	4.1 ± 0.7	1.3	0.4 ± 0.1	1.4
K147A	86 ± 10	14 ± 2	1.1	0.4 ± 0.1	2.1
K149A	55 ± 6	8.6 ± 1.0	1.1	0.4 ± 0.1	1.8

[a] The dissociation constants of methionine (met) were derived from spectrophotofluorimetric titrations of each variant studied. [b] K_{met} is the dissociation constant of the enzyme:methionine complex. [c] K_{met}^{ado} is the apparent dissociation constant of methionine when measured in the presence of 9.4 mM adenosine. [d] $C_{met}^{ado} = RT \text{ Log}(K_{met}/K_{met}^{ado})$. [e] K_{met}^{adoPP} is the apparent dissociation constant of methionine when measured in the presence of both 9.4 mM adenosine and 2 mM PPi−$MgCl_2$. [f] $C_{met}^{adoPP} = RT \text{ Log}(K_{met}^{ado}/K_{met}^{adoPP})$.

Table 4: Equilibrium Parameters of the Binding of Methioninol and $tRNA_m^{Met}$ to the Variants of Methionyl-tRNA Synthetase[a]

	K_{metol} (μM)[b]	K_{metol}^{ATP}(μM)[c]	C_{metol}^{ATP}(kcal/mol)[d]	K_{tRNA} (μM)[e]
M547	500 ± 40	2.7 ± 0.2	3.1	1.4 ± 0.4
F135L	70 ± 5	1.3 ± 0.7	2.4	1.4 ± 0.8
D138A	2200 ± 600	130 ± 20	1.6	0.7 ± 0.1
D138N	2100 ± 600	60 ± 10	2.1	0.55 ± 0.08
R139A	1150 ± 200	110 ± 20	1.4	2.5 ± 2.0
R139K	1300 ± 200	70 ± 15	1.7	1.2 ± 0.7
F140L	1450 ± 200	20 ± 6	2.5	1.4 ± 0.9
K142Q	200 ± 10	2.6± 0.6	2.6	1.0 ± 0.2
K147A	560 ± 35	4.8 ± 1.2	2.8	2.1 ± 0.3
K149A	450 ± 40	3.7 ± 0.9	2.8	2.1 ± 0.3

[a] The dissociation constants of methioninol (metol) or of $tRNA_m^{Met}$ (tRNA) were derived from spectrophotofluorimetric titrations of each variant studied. [b] K_{metol} is the dissociation constant of the enzyme:methioninol complex. [c] K_{metol}^{ATP} is the apparent dissociation constant of methioninol when measured in the presence of 8 mM ATP−Mg^{2+}. [d] $C_{metol}^{ATP} = RT \text{ Log}(K_{metol}/K_{metol}^{ATP})$. [e] K_{tRNA} is the dissociation constant of the eEnzyme:$tRNA^{Met}_m$ complex.

whereas the binding of methioninol was determined in the presence of ATP−Mg^{2+} (Tables 3 and 4). When the pyrophosphate moiety of the ATP molecule was involved (*i.e.*, effect of PPi−Mg^{2+} on the binding constant of methionine in the presence of adenosine or effect of ATP−Mg^{2+} on the binding constant of methioninol), the positive couplings between the ligand-binding sites of the mutant enzymes decreased in strength as compared to the case of M547. Indeed, the gain of coupling normally observed when comparing the combination of methionine and adenosine with that of methionine and adenosine plus PPi−Mg^{2+} almost disappeared with the variants at positions 138 and 139.

Finally, measurement of the values of the dissociation constants of the complexes formed by the mutant enzymes with $tRNA_m^{Met}$ showed that none was modified by a factor greater than 3, even in the case of the F135L enzyme, which was, however, affected in the efficiency of the tRNA aminoacylation reaction (Table 4).

It was therefore clear that the disfunction of the enzymes modified at position 138 or 139 was not the consequence of an inability to bind one among the three substrates (methionine, ATP, tRNA). Moreover, although no direct proof insured that the mutant and wild type enzymes are isomorphic, the above results indicated that no major structural change of the active site occurred upon the introduced mutations. On another hand, these enzymes were deeply affected at the level of the intensity of the coupling developed between the pyrophosphate site and the methionine and adenosine sites upon the formation of the E:Met:Ado:PPi−Mg^{2+} complex. Since the latter complex is thought to mimic the transition state complex (Blanquet et al., 1975; Hyafil et al., 1976), it was of interest to study directly the stabilization of the transition state in the methionine activation reaction sustained by the D138 or R139 variants.

(C) Residues Asp138 and Arg139 Are Involved in Methionyl Adenylate Formation. The rates of interconversion between the E:Met:ATP−Mg^{2+} and E:methionyl adenylate:PPi−Mg^{2+} complexes (k_f and k_b as defined in Scheme 1) were determined by using the fluorescence-monitored stopped-flow technique (Hyafil et al., 1976). With the D138A and R139A variants, the rates of formation of methionyl adenylate were slowed down by 2 and 4 orders of magnitude, respectively, as compared to wild type M547 enzyme (Table 5). In contrast, in each case, the affinity of ATP−Mg^{2+} for the E:Met complex was not modified (Table 5).

In the cases of the D138A and D138N variants, the rates of reversion of methionyl adenylate by PPi−Mg^{2+} were decreased by factors of 20 and 3, respectively, and the affinity of PPi−Mg^{2+} for the E:methionyl adenylate complex was slightly reduced. In the case of the R139A mutant, saturation of the enzyme:adenylate complex by PPi−Mg^{2+} was not possible, indicating that the pyrophosphate affinity was reduced by at least 2 orders of magnitude. This precluded the determination of k_b but not that of $k_b/K_{PP}^{Met\sim AMP}$, which was reduced by 4 orders of magnitude as compared to M547. Interestingly, the affinity constant of PPi−Mg^{2+} for the E:methionyl adenylate complex corresponding to the R139K variant remained measurable. Its value was lowered by a factor of 10 as compared to the situation with the M547 enzyme. The k_b rate was, in this case, slowed down 100-fold.

DISCUSSION

(A) The Sequence Upstream from the Cys Motif Is Essential for MetRS Activity. The mutations introduced at positions 138 and 139 strongly impair the rate of methionyl adenylate formation while slightly affecting the ability to form the ternary complex E:Met:ATP−Mg^{2+}. Therefore residues D138 and R139, located upstream from the Cys motif, appear to participate to the stabilization of the transition state of the activation reaction. Figure 3 compares the energetic profiles of the amino acid activation reactions catalyzed by the D138A, D138N, R139A, and R139K variants to the case of wild type M547.

The large loss of affinity of PPi−Mg^{2+} for the R139A:methionyl adenylate complex supports the involvement of an electrostatic interaction between the guanidinium of R139 and the pyrophosphate moiety of ATP during the reaction. Accordingly, when a lysine residue is introduced at position 139 (R139K mutant), increases of the PPi−Mg^{2+} affinity and of the rate of methionyl adenylate synthesis are observed, as compared to the R139A variant. However, catalytic properties identical to those of the wild type enzyme are not

Table 5: Parameters of the Reaction of Formation of Methionyl Adenylate Catalyzed by the Variants of MetRS[a]

	M547	D138A	D138N	R139A	R139K
k_f (s^{-1})	350 ± 50	0.9 ± 0.1	7.7 ± 0.9	0.016 ± 0.003	0.26 ± 0.03
K_{ATP}^{Met} (mM)	1.0 ± 0.2	0.3 ± 0.1	0.45 ± 0.15	2.4 ± 1	2.6 ± 0.5
k_f/K_{ATP}^{Met} (s^{-1} M^{-1}) × 10^{-3}	350 ± 120	3.0 ± 1.3	17 ± 8	0.007 ± 0.0040	0.10 ± 0.03
k_b (s^{-1})	180 ± 20	9.4 ± 1.2	65 ± 5	nm	1.6 ± 0.4
$K_{PP}^{Met\sim AMP}$ (mM)	0.06 ± 0.02	0.17 ± 0.03	0.22 ± 0.02	>5	0.6 ± 0.3
$k_b/K_{PP}^{Met\sim AMP}$ (s^{-1} M^{-1}) × 10^{-3}	3000 ± 1330	55 ± 17	295 ± 50	0.080 ± 0.007	2.7 ± 2

[a] In the case of the backward reaction, the methionyl adenylate was preformed in the presence of 0.1 mM ATP−Mg^{2+} for the M547 enzyme, 50 μM ATP for the D138A and D138N enzymes, and 0.5 mM ATP−Mg^{2+} for the R139A and R139K enzymes.

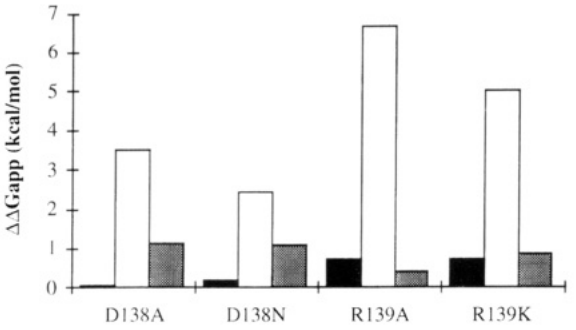

FIGURE 3: Difference free energy diagram for the M547 variants studied. The difference free energies ($\Delta\Delta G_{app}$) for each step of the methionine activation reaction was calculated by substracting the free energy of the M547 enzyme complex from the free energy of the indicated mutant enzyme complex ("E" refers to "enzyme"). Filled bars, E:Met complex; open bars, E:Met:ATP−Mg^{2+} ground state complex; dark grey bars, E:Met:ATP−Mg^{2+} transition state complex; light grey bars, E:methionyl adenylate complex.

restored (Figure 3). The role of R139 would therefore resemble that of the basic residues of the KMSKS region of MetRS which stabilize the transition state complex through interactions with the phosphate chain of the ATP molecule (Mechulam et al., 1991; Schmitt et al., 1994).

The D138 residue also is involved in the stabilisation of the transition state of the reaction, although its substitution has less consequence than that of R139. Notably, the affinity of PPi−Mg^{2+} for the D138A:methionyl adenylate complex was only slightly modified, while methionine affinity was significantly decreased. One possible explanation is that, provided it is close to the active site crevice (see below), the negatively charged side chain of D138 interacts with the amino group of the methionine substrate.

(B) Zinc Ion Has a Structural Role. The NMR structure of the isolated zinc-binding site of MetRS (peptide 138−163) is composed of four consecutive tight turns (Fourmy et al., 1993a). The second and fourth turns carry the four cysteines, through which the zinc atom is ligated. Residues D138 and R139 are located immediately upstream from the first turn, which involves residues 142−144. As previously mentioned (Fourmy et al., 1993a), the corresponding region of the MetRS crystallographic structure (Brunie et al., 1990) is currently being revised. However, the tentative grafting of the NMR structure of the isolated zinc-binding peptide onto the available crystallographic structure of the whole enzyme suggests that D138 and R139 might be close to the active site crevice (Figure 1). Such a location would account fo direct involvement of these residues in catalysis. In addition, the removal of zinc can be predicted to cause a displacement of the D138 and R139 residues because the four tight turns stabilized by this metal would be opened. Indeed, the behavior in the catalysis of the variants at position 138 and 139 is quite similar to that of the variants of the Cys motif, in which either cysteine was substituted by an alanine (Fourmy et al., 1993b).

A structural role of zinc in MetRS is also supported by the consequence of the conservative substitution of F140 into leucine. Such a modification of the hydrophobic core close to the tetracoordination site of the zinc atom causes a moderate but significant perturbation of the catalytic parameters.

(C) Zinc-Binding Peptide Is Involved in the Aminoacylation of tRNA. The specificity of tRNA aminoacylation by MetRS is dominated by the binding of the anticodon of tRNA to a region of the enzyme surrounding the Trp461 residue (Ghosh et al., 1990; Meinnel et al., 1991; Schmitt et al., 1993). However, base 73 and base pairs 2−71 and 3−70 in the acceptor stem of $tRNAs^{Met}$ were also found to be important for full aminoacylation efficiency (Meinnel et al., 1993). Mutations of the latter nucleotides in $tRNA_f^{Met}$ led to tRNA species being less rapidly methionylated but retaining full affinity for MetRS. From this, it was concluded that the acceptor stem of $tRNAs^{Met}$ participates in the productive positioning of the 3′-terminal adenosine of tRNA with respect to the catalytic center of MetRS. Reciprocally, enzyme residues involved in such positioning are also likely to be found. In the present study, mutation of F135 into leucine strongly modifies both the $K_m$value of $tRNA_m^{Met}$ and the V_m value of the aminoacylation reaction without significantly altering the affinity of the variant enzyme for tRNA. In turn, mutations of D138 into alanine or asparagine lead to a significant increase of the affinity of $tRNA_m^{Met}$, thereby indicating that the D138 side chain lies in the vicinity of the tRNA acceptor arm. Therefore, a short sequence upstream from the zinc-binding peptide of *E. coli* MetRS and comprising F135 and D138 appears involved in the orientation of the 3′ end of tRNA during methionine transfer. In the case of D138, this might occur through electrostatic repulsion of the phosphate backbone of tRNA.

Interestingly, in the case of the *E. coli* AlaRS, a class 2 enzyme, residues located immediately upstream from the Cys/His zinc-binding motif were found to be important for the efficiency of $tRNA^{Ala}$ aminoacylation (Miller & Schimmel, 1992).

(D) Zinc-Binding Peptide of aaRS: An Additional Module in the Catalytic Domain Which Is Important for Amino Acid Activation and/or tRNA Aminoacylation and Recognition. In the cases of all zinc containing aaRS characterized until now (AlaRS, IleRS, GluRS, MetRS, and ThrRS from *E. coli*, and MetRS and IleRS from *Thermus thermophilus*), the zinc-free apoenzyme or the enzyme species in which the Cys/His motif could be deleted were shown to be inactive (Fourmy et al., 1993b; Landro & Schimmel, 1993; Liu et al., 1993; Miller et al., 1991a; Nureki et al., 1993; Starzyk

et al., 1987). Zinc appears therefore essential to the activity of those aaRS which contain this metal.

In the case of MetRS, the zinc-binding site is likely to behave as a module in the 3-D structure with a conformation resembling that of the nucleocapsid protein NCp7 of HIV, another RNA-binding protein (Morellet et al., 1992).

Notably, the superimposition of the MetRS and GlnRS structures (Perona et al., 1991) indicates that the zinc-binding peptide of MetRS is spatially equivalent to the tRNA acceptor arm binding domain of GlnRS (Figure 1). The crystal structure of the GlnRS:ATP:$tRNA^{Gln}$ complex revealed that parts of the acceptor binding domain, which is located inside the connective polypeptide 1 of the Rossmann fold, interact with the acceptor stem of $tRNA^{Gln}$ (Rould et al., 1989). Numerous basic residues of this acceptor binding domain (Arg133 and Arg192, for instance) guide the ribose–phosphate backbone of the tRNA toward the active site. In addition, the Arg130 and Glu131 residues carried by the acceptor binding domain of GlnRS are important for the specificity of the aminoacylation reaction (Weygand-Durasevic et al., 1993). In the case of the TyrRS from *Bacillus stearothermophilus*, an acidic residue of the connective polypeptide 1, Glu152, was found to be involved in the recognition of the acceptor stem of $tRNA^{Tyr}$ (Vidal-Cros & Bedouelle, 1992). These data strongly indicate that residues belonging to the connective polypeptide 1 might generally participate to the guiding of the acceptor stem of tRNA toward the catalytic center of class 1 aaRS. Following the same idea, the zinc-binding site of *E. coli* GluRS was mapped in a region corresponding to the GlnRS acceptor binding peptide involved in tRNA recognition, *i.e.*, in the connective polypeptide 1 (Breton et al., 1990). This correspondence suggests that the zinc-binding peptide of GluRS might be, like that of MetRS, in the vicinity of the active site and involved in tRNA aminoacylation. Finally, one of the two zinc ions complexed to IleRS is liganded by two residues belonging to connective polypeptide 1 (Landro et al., 1994).

In the case of AlaRS, a class 2 enzyme, the zinc-binding motif is carried on a peptide inserted between motifs 2 and 3 (Pouplana et al., 1993). This region is believed to be involved in tRNA recognition (Miller et al., 1991b; Miller & Schimmel, 1992). Interestingly, in the case of the class 2 AspRS from *Saccharomyces cerevisiae*, a module inserted between motifs 2 and 3 is shown important for the recognition of $tRNA^{Asp}$ (Cavarelli et al., 1993); this module does not, however, contain zinc. A similar but larger α/β-structured connective polypeptide was also identified in AspRS of *T. thermophilus* (Poterszman et al., 1993). This polypeptide adopts a 3-D conformation analogous to that of a phosphate-binding protein and is believed to be involved in tRNA recognition (Delarue et al., 1994).

In conclusion, the occurrence of variable connective polypeptides between two conserved secondary structure elements of the catalytic domain of aaRS may have been a way to introduce diversity among the active sites during evolution. These insertions appear to have occurred either between the two halves of the nucleotide binding fold of class 1 aaRS or between motifs 2 and 3 of the catalytic domain of class 2 enzymes. The appearance within such connective polypeptides of zinc-binding sites may have added constraints to the 3-D structure of the inserted elements and/or increased their diversity. Clearly, these inserted elements nowadays strongly contribute through crucial residues to both the amino acid activation reaction and the guiding of the 3′ end of tRNA.

ACKNOWLEDGMENT

We thank Pr. J. D. Puglisi and Drs. T. Meinnel and E. Schmitt for helpful advice and critical reading of the manuscript.

REFERENCES

Berg, J. M. (1990) *J. Biol. Chem. 265*, 6513–6516.
Blanquet, S., Fayat, G., Waller, J.-P., & Iwatsubo, M. (1972) *Eur. J. Biochem. 24*, 461–469.
Blanquet, S., Iwatsubo, M., & Waller, J.-P. (1973) *Eur. J. Biochem. 36*, 213–226.
Blanquet, S., Fayat, G., & Waller, J.-P. (1974) *Eur. J. Biochem. 44*, 343–351.
Blanquet, S., Fayat, G., & Waller, J.-P. (1975) *J. Mol. Biol. 94*, 1–15.
Breton, R., Watson, D., Yaguchi, M., & Lapointe, J. (1990) *J. Biol. Chem. 265*, 18248–18255.
Brick, P., Bhat, T. N., & Blow, D. M. (1989) *J. Mol. Biol. 208*, 83–98.
Brunie, S., Zelwer, C., & Risler, J.-L. (1990) *J. Mol. Biol. 216*, 411–424.
Cassio, D., & Waller, J.-P. (1971) *Eur. J. Biochem. 20*, 283–300.
Cavarelli, J., Rees, B., Ruff, M., Thierry, J. C., & Moras, D. (1993) *Nature* (London) *362*, 181–184.
Cusack, S., Härtlein, M., & Leberman, R. (1991) *Nucleic Acids Res. 19*, 3489–3498.
Dardel, F. (1994) *Comput. Appl. Biosci. 10*, 273–275.
Dardel, F., Fayat, G., & Blanquet, S. (1984) *J. Bacteriol. 160*, 1115–1122.
Delarue, M., Poterszman, A., Nikonov, S., Garber, M., Moras, D., & Thierry, J. C. (1994) *EMBO J. 13*, 3219–3229.
Eriani, G., Delarue, M., Poch, O., Gangloff, J., & Moras, D. (1990) *Nature* (London) *347*, 203–206.
Fayat, G., Fromant, M., & Blanquet, S. (1977) *Biochemistry 16*, 2570–2579.
Fourmy, D., Dardel, F., & Blanquet, S. (1993a) *J. Mol. Biol. 231*, 1078–1089.
Fourmy, D., Meinnel, T., Mechulam, Y., & Blanquet, S. (1993b) *J. Mol. Biol. 231*, 1068–1077.
Ghosh, G., Pelka, H., & Schulman, L. H. (1990) *Biochemistry 29*, 2220–2225.
Ghosh, G., Brunie, S., & Schulman, L. H. (1991) *J. Biol. Chem. 266*, 17136–17141.
Hirel, P.-H., Lévêque, F., Mellot, P., Dardel, F., Panvert, M., Mechulam, Y., & Fayat, G. (1988) *Biochimie (Paris) 70*, 773–782.
Hyafil, F., Jacques, Y., Fayat, G., Fromant, M., Dessen, P., & Blanquet, S. (1976) *Biochemistry 15*, 3678–3685.
Kraulis, P. (1991) *J. Appl. Crystallogr. 24*, 946–950.
Landro, J. A., & Schimmel, P. (1993) *Proc. Natl. Acad. Sci. U.S.A. 90*, 2261–2265.
Landro, J. A., & Schimmel, P. (1994) *J. Biol. Chem. 269*, 20217–20220.
Landro, J. A., Schmidt, E., Schimmel, P., Tierney, D. L., & Penner-Hahn, J. E. (1994) *Biochemistry 33*, 14213–14220.
Lawrence, F., Blanquet, S., Poiret, M., Robert-Gero, M., & Waller, J.-P. (1973) *Eur. J. Biochem. 36*, 234–243.
Liu, J. H., Lin, S., Blochet, J., Pézolet, M., & Lapointe, J. (1993) *Biochemistry 32*, 11390–11396.
Mayaux, J.-F., & Blanquet, S. (1981) *Biochemistry 20*, 4647–4654.
Mayaux, J.-F., Kalogerakos, T., Brito, K. K., & Blanquet, S. (1982) *Eur. J. Biochem. 128*, 41–46.
Mechulam, Y., Dardel, F., LeCorre, D., Blanquet, S., & Fayat, G. (1991) *J. Mol. Biol. 217*, 465–475.
Mechulam, Y., Meinnel, T., & Blanquet, S. (1995). Aminoacyl-tRNA synthetases: a class of RNA binding enzymes, in *Subcellular biochemistry* (Biswas, B. B., & Roy, S., Eds.) Vol. 24, pp 323–376, Plenum Press, New York.

Meinnel, T., Mechulam, Y., LeCorre, D., Panvert, M., Blanquet, S., & Fayat, G. (1991) *Proc. Natl. Acad. Sci. U.S.A. 88*, 291−295.

Meinnel, T., Mechulam, Y., & Fayat, G. (1988) *Nucleic Acids Res. 16*, 8095−8096.

Meinnel, T., Mechulam, Y., Lazennec, C., Blanquet, S., & Fayat, G. (1993) *J. Mol. Biol. 229*, 26−36.

Meinnel, T., Mechulam, Y., & Blanquet, S. (1995). Aminoacyl-tRNA synthetases: occurrence, structure and function, In *tRNA: Stucture, Biosynthesis and Function* (Söll, D., & RajBhandary, U., Eds.) pp 251−292, American Society for Microbiology, Washington, DC.

Mellot, P., Mechulam, Y., LeCorre, D., Blanquet, S., & Fayat, G. (1989) *J. Mol. Biol. 208*, 429−443.

Miller, W. T., Hill, K. A. W., & Schimmel, P. (1991a) *Biochemistry 30*, 6970−6976.

Miller, W. T., Hou, Y.-M., & Schimmel, P. (1991b) *Biochemistry 30*, 2635−2641.

Miller, W. T., & Schimmel, P. (1992) *Proc. Natl. Acad. Sci. U.S.A. 89*, 2032−2035.

Morellet, N., Jullian, N., De Rocquigny, H., Maigret, B., Darlix, J. L., & Roques, B. P. (1992) *EMBO J. 11*, 3059−3065.

Nureki, O., Khono, T., Sakamoto, K., Miyazawa, T., & Yokoyama, S. (1993) *J. Biol. Chem. 268*, 15368−15373.

Perona, J. J., Rould, M. A., Steitz, T. A., Risler, J.-L., Zelwer, C., & Brunie, S. (1991) *Proc. Natl. Acad. Sci. U.S.A. 88*, 2903−2907.

Posorske, L. H., Cohn, M., Yanagisawa, N., & Auld, D. S. (1979) *Biochim. Biophys. Acta 576*, 128−133.

Poterszman, A., Plateau, P., Moras, D., Blanquet, S., Mazauric, M., Kreutzer, R., & Kern, D. (1993) *FEBS Lett. 325*, 183−186.

Pouplana, L. R., Buechter, D. D., Davis, M. W., & Schimmel, P. (1993) *Protein Sci. 2*, 2259−2262.

Rossmann, G. M., Moras, D., & Olsen, K. W. (1974) *Nature 250*, 194−199.

Rould, M. A., Perona, J. J., Söll, D., & Steitz, T. A. (1989) *Science 246*, 1135−1142.

Schmitt, E., Meinnel, T., Panvert, M., Mechulam, Y., & Blanquet, S. (1993) *J. Mol. Biol. 233*, 615−628.

Schmitt, E., Meinnel, T., Blanquet, S., & Mechulam, Y. (1994) *J. Mol. Biol. 242*, 566−577.

Starzyk, R. M., Webster, T. A., & Schimmel, P. (1987) *Science 237*, 1614−1618.

Vidal-Cros, A., & Bedouelle, H. (1992) *J. Mol. Biol. 223*, 801−810.

Walter, P., Gangloff, J., Bonnet, J., Boulanger, Y., Ebel, J.-P., & Fasiolo, F. (1983) *Proc. Natl. Acad. Sci. U.S.A. 80*, 2437−2441.

Weygand-Durasevic, I., Schwob, E., & Söll, D. (1993) *Proc. Natl. Acad. Sci. U.S.A. 90*, 2010−2014.

BI951566G